Biochemistry and Biophysics Reports 38 (2024) 101744

Contents lists available at ScienceDirect

Biochemistry and Biophysics Reports

journal homepage: www.elsevier.com/locate/bbrep

Blockage of TMEM189 induces G2/M arrest and inhibits the growth of breast tumors

Song Chen [1], Meng Tie [1], Mengyue Wu, Anyuan He [**], Yali Chen [*]

School of Life Sciences, Anhui Medical University, Hefei, China

A B S T R A C T

Cancer is the major cause of premature death in humans worldwide, demanding more efficient therapeutics. Aberrant cell proliferation resulting from the loss of cell cycle regulation is the major hallmark of cancer, so targeting cell cycle is a promising strategy to combat cancer. However, the molecular mechanism underlying the dysregulation of cell cycle of cancer cells remains poorly understood. TMEM189, a newly identified protein, plays roles in the biosynthesis of ethanolamine plasmalogen and the regulation of autophagy. Here, we demonstrated that the expression level of TMEM189 was negatively correlated with the survival rate of the cancer patients. TMEM189 deficiency significantly suppresses the cancer cell proliferation and migration, and causes cell cycle G2/M arrest both *in vitro* and *in vivo*. Furthermore, TMEM189 depletion suppressed the growth of breast tumors *in vivo*. Taken together, our work indicated that TMEM189 promotes cancer progression by regulating cell cycle G2/M transition, suggesting that it is a promising target in cancer therapy.

1. Introduction

Cancer is the leading cause of premature death in humans worldwide, which necessitates the development of improved and more efficient therapeutic strategies [1,2]. Through genome reprogramming, cancer cells gain multiple capabilities that are essential for their ability to survive and proliferate in a stressful tumor microenvironment. Those capabilities include immune cell resistance, transcriptional dysregulation, lipid metabolism imbalance, cell cycle dysregulation, and so on [1,3]. The development of new treatments targeting those cancer features could bring out novel therapeutics for cancer patients.

Indeed, aberrant cell proliferation resulting from the loss of cell cycle regulation is the major characteristic of cancer [4–6]. Cell cycle or cell division is a series of events occurring in a cell that causes a mother cell to divide into two daughter cells. The cell cycle is divided into four sequential phases, namely G1 (Gap 1), S (synthesis), G2 (Gap 2), and M (mitosis). Several specific cell cycle checkpoints tightly control the proliferation of cells through these various phases [7]. Although persistent efforts have been made to investigate the dysregulation of cancer cell cycle, the underlying mechanism remains poorly understood.

TMEM189 (transmembrane protein 189), a newly identified protein, is a highly conserved protein and is expressed in numerous types of tissues and cells [8]. It has been reported that TMEM189 could catalyze the biosynthesis of ethanolamine plasmalogen through the insertion of the alk-1′-enyl ether or 'vinyl-ether' double bond to plasmanylethanolamines [9]. Interestingly, TMEM189 could negatively regulate autophagy through its direct interaction with ULK1 [10], indicating that TMEM189 might have extra functions in addition to its plasmalogen synthetic activity. However, the role of TMEM189 in the progression of cancer remains unclear.

In the present study, we demonstrated that TMEM189 expression level was negatively correlated with the survival rate of breast, liver, and renal cancer patients. TMEM189 knockdown significantly suppresses the proliferation and migration of liver and breast cancer cells, and causes cell cycle G2/M arrest *in vitro*. Furthermore, the knockdown of TMEM189 suppresses the growth of breast tumors *in vivo*. Taken together, our work indicated that TMEM189 was a promising target in cancer treatment.

2. Materials and methods

2.1. Plasmids and lentivirus packaging

The plasmid pLKO.1 was used as a backbone to clone plasmids expressing shRNA with a standard protocol [11]. The shRNA sequences were as follows: 5′-CGA CAT GAA ATG GGC ACA GAA-3′ (#1) and 5′-GCA TGA CTT CAT CGA GAC CAA-3 ′ (#2) for mouse TMEM189, 5′-GCA TCA CCA CAG GCT GGC TCA-3′ (#1) and 5′-CTC GGG CAG ATG

* Corresponding author.
** Corresponding author.
E-mail addresses: heanyuan85@foxmail.com (A. He), yalichen0519@ahmu.edu.cn (Y. Chen).
[1] these authors contributed equally.

https://doi.org/10.1016/j.bbrep.2024.101744
Received 31 August 2023; Received in revised form 8 May 2024; Accepted 27 May 2024

ACA TGA AAT-3′ (#2) for human TMEM189, and 5′-CCT AAG GTT AAG TCG CCC TCG-3′ for scramble (negative control). The EGFP of pLJM1-EGFP (addgene #19319) was replaced with TMEM189 to generate a pLJM1-hTMEM189 plasmid by using in-fusion cloning (YEASEN, China). All plasmids were prepared by using the Plasmid Midi Kit (TIANGEN, China). MD2.G, Pspax, and the transfer plasmid were co-transfected into HEK293T cell to package lentivirus by using a Liposomal Transfection Reagent (YEASEN, China). Viruses were collected 48–72 h after transfection and stored at −80 °C until use.

2.2. Cell culture

4T1 and MCF-7 cells were gifted by Yong Zhu (Anhui Medical University, Anhui, China). HEK293T and Capan-1 cells were gifted by Daoxiang Zhang (Anhui Medical University, Anhui, China). HepG2 and Hepa1-6 cells were gifted by Hong Zhou (Anhui Medical University, Anhui, China). All cell lines were maintained at 37 °C and 5 % CO_2, which were cultured in Dulbecco's modified Eagle's medium (Gibco) supplemented with 10 % fetal bovine serum (HyClone) and 100 IU penicillin and 100 mg/mL streptomycin (P/S). The cells infected with lentivirus were selected with puromycin for at least 4 days.

2.3. Animal experiment

Female BALB/c mice aged 7–8 weeks were used in all animal experiments. All mice were housed in a pathogen-free environment with a 12-h light/12-h dark cycle. Animals have free access to water and food (normal chow diet). The corresponding cells were subcutaneously injected on both sides of the dorsum of the BALB/c mice in a total volume of 100 μL (2×10^4 cells/mouse), a similar cell number was used by Lu et al. [12]. One week post-injection, tumor volumes were measured every 3 days (tumor volume = $\text{width}^2 \times \text{length} \times 1/2$), and body weights were measured twice a week till sacrifice. Mice were sacrificed 22 days after the cell inoculation, at which time the tumors were excised, weighed, and analyzed. All animal experiments were approved by and performed following the guidelines of the animal ethics committees of Anhui Medical University.

2.4. Cell cycle analysis by FACS assays

Cell cycle analyses have been performed as previously described [13], briefly, adherent cells were cultured in serum-free medium for 12h to synchronize all the cells at the G0 phase, and then changed to normal media for another 24h. Cells were harvested as a single cell suspension by trypsin treatment, fixed with 70 % ethanol, collected by centrifugation, and washed with PBS. Cells were resuspended in 500 mL PBS containing propidium iodide (PI) (50 mg/mL), and DNase-free RNase (10 μg/mL, Vazyme), and then incubated at 4 °C for 0.5 h. Samples were analyzed by flow cytometry (Cytoflex S, Beckman, Germany) and cell cycle analyses were performed by FlowJo_V10. software.

2.5. Cell viability measured by CCK8 assay

Cell viability assays were performed using the Cell Counting Kit-8 (CCK8) (Biosharp, China) according to the manufacturer's instructions. Briefly, cells were plated in triplicate at 500 cells/well, and cultured in a complete culture medium for 48 h in 96-well plates. Absorbance at 450 nm was measured on SPARK Cyto (TECAN, Switzerland). Cell viability was calculated as follows: cell viability = absorbance of test group/absorbance of control cell group × 100 %. Each experiment was performed in biological triplicate and independently repeated 3 times.

2.6. Cell colony formation assay

For the colony formation assay, cells were plated in triplicate at 1000 cells/well, and cultured for 10 days in 6-well plates. Then cells were fixed with 4 % paraformaldehyde for 15 min and stained with 0.25 % crystal violet for 15 min. Colonies were counted and photographed.

2.7. Wound healing assay

Cells were cultured in 6-well plates with a culture medium containing 10 % FBS and grown to a nearly confluent cell monolayer. A linear wound was made by scratching the center of the well with a 10 μL plastic pipette tip. Cells were washed with PBS 3 times to remove detached cells and the remaining cells were maintained in the serum-free medium for 48 h. The gap distance of the wound was photographed by using an inverted phase contrast microscope (Carl Zeiss, Germany) and measured by Image-J.

2.8. Transwell assay

The invasion of cancer cells was evaluated by a Matrigel-coated Transwell chamber (Corning, MA, USA). In short, cells were trypsinized, washed, and seeded at 2×10^4 cells/well onto the upper chamber, with the lower chamber filled with culture medium supplemented with 10 % FBS. After 20 h incubation, the cells on the top surface of the chamber were rubbed off, while the cells on the lower surface were fixed with 4 % paraformaldehyde for 15 min and stained with 0.25 % crystal violet for 15 min. Then four random fields of every chamber were scanned to record the cells at the lower membrane side at 4 ×, 10 ×, and 20 × magnifications using an inverted phase contrast microscope (Carl Zeiss, Germany).

2.9. Immunohistochemistry (IHC) assay

Tumor samples were fixed in 4 % formaldehyde, dehydrated, embedded, and cut into 5 μm sections. After antigen retrieval, sections were incubated in H_2O_2 solution, washed, and incubated with primary antibody against Ki67 (1:100, Abcam) for 12 h. Sections were then incubated with HRP-conjugated secondary antibody (1:400, Thermo Fisher Scientific). DAB substrate was added to detect the signal, followed by hematoxylin staining. Finally, images were captured under a microscope (Carl Zeiss, Germany).

2.10. Quantitative real-time PCR

Total RNA from cells or tissues was extracted using TRIzol® Reagent (Vazyme Biotech). Complementary DNA was synthesized using HiScript II Reverse Transcriptase (Vazyme Biotech) according to the manufacturer's instructions. QPCR was performed using SYBR qPCR Master Mix (Vazyme Biotech) on StepOnePlusTM Real-Time PCR Systems. L32 was used as an internal reference. Primer sequences are provided in Supplementary Table 1.

2.11. Western blotting

Cells were lysed with RIPA buffer and the proteins were extracted with a standard protocol. Forty μg protein for each sample was loaded for western blotting. Antibodies were as follows: TMEM189 (A8380, Abclonal), Tubulin (AF0001, Beyotime), Cyclin B1 (R23324, Zenbio), CDK1 (R23884, Zenbio), pCDK1 (310063, Zenbio).

2.12. Transcriptomic analysis

Cell samples were harvested and delivered to Oebiotech Company (Shanghai, China) for the transcriptomic analysis based on the Illumina Seq method. Raw reads were banked at the National Center for Biotechnology Information's Sequence Read Archive under accession no. PRJNA897884. Differential expression analysis was performed using the DESeq2 [14]. Genes with Q value ≤ 0.05, DEGs with $|\log_2 FC| > 1$,

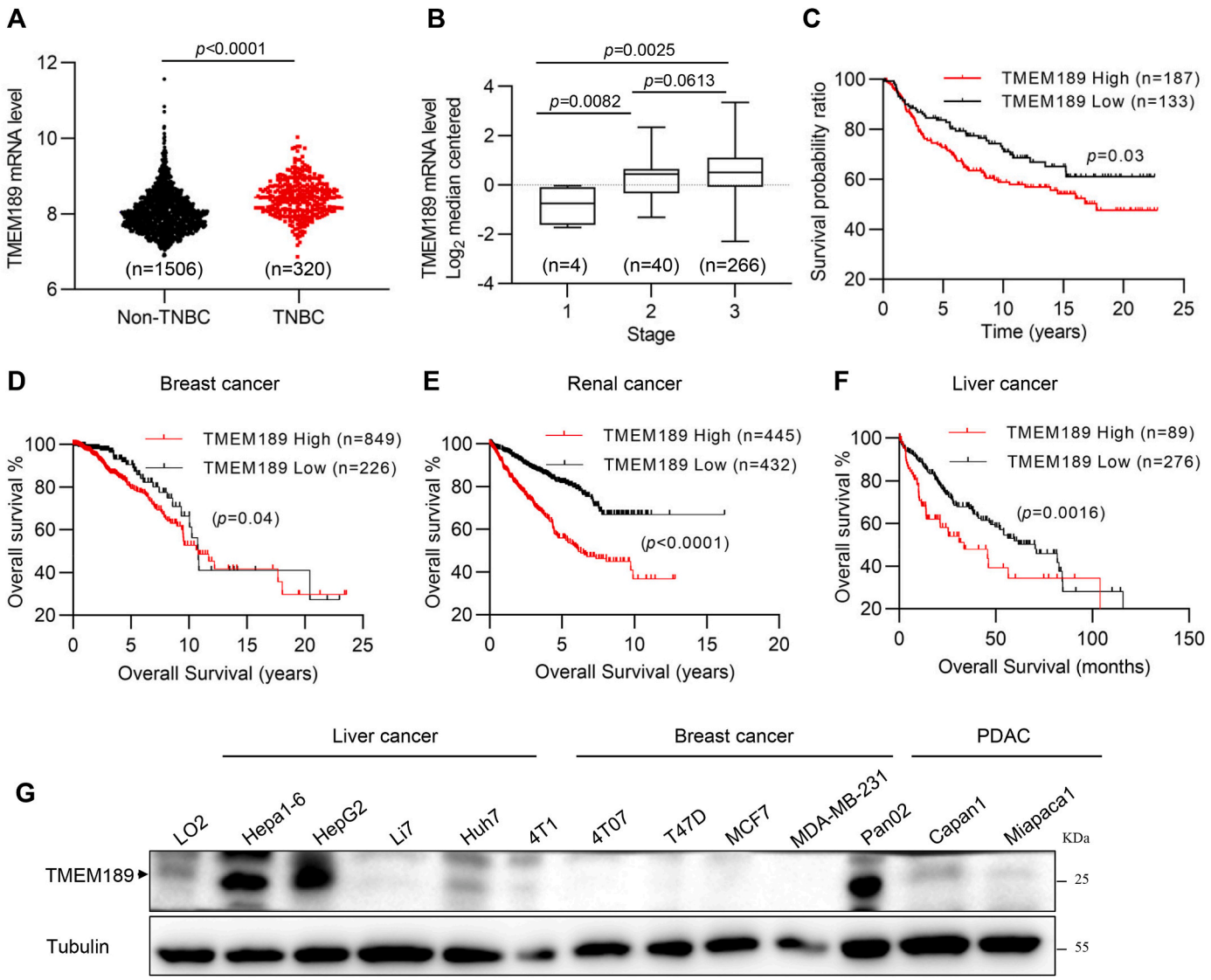

Fig. 1. TMEM189 expression level is associated with cancer malignancy

(A) TMEM189 mRNA levels of TNBC and non-TNBC patients's tumor tissues from the Metabric datasets. (B) TMEM189 mRNA levels in three tumor stages of TNBC samples from the Metabric dataset. (C) The overall survival probability analysis for 320 TNBC patients from the Metabric dataset by TMEM189 mRNA level. (D–F) Overall survival analysis of The Human Protein Atlas cohorts of patients with breast, renal, and liver cancer. (G) Western blotting analysis for TMEM189 expression in various breast, liver, and pancreatic cancer cell lines. $*p < 0.05$, $**p < 0.01$ and $***p < 0.001$.

and Q value ≤ 0.05 were considered to be significantly differentially expressed. In addition, GO functional enrichment analysis was carried out by Goatools (https://github.com/tanghaibao/Goatools).

2.13. Statistical analysis

Data analyses were performed using GraphPad Prism 8.0. The data presentation (mean ± SEM) and statistical analyses were described in the figure legends. p-value <0.05 was considered as a statistically significant difference. The statistical details of experiments can be found in the figure legends, figures, and text of the Results.

3. Results

3.1. High TMEM189 level is correlated with a poor outcome in multiple cancers

To investigate the role of TMEM189 in cancer progression, we first evaluated the correlation between TMEM189 expression level and cancer progression using the Metabric dataset. Triple-negative breast cancer (TNBC) is an aggressive and heterogeneous subtype of breast cancer with a highly invasive nature [2]. In this dataset, there were 320 TNBC samples and 1506 non-TNBC samples. By comparison, TMEM189 mRNA levels of TNBC patient samples were remarkably higher than those of non-TNBC samples (Fig. 1A). More importantly, high TMEM189 mRNA level was correlated with poor tumor stage (Fig. 1B) and poor disease-free survival (DFS) (Fig. 1C).

Furthermore, TMEM189 protein levels were negatively correlated with the overall survival of patients with breast, liver, and renal cancer, suggesting that tumor malignancy is closely related to TMEM189 expression level (Fig. 1D–F). Besides, we found that TMEM189 protein levels were varied in different cancer cells and were highly expressed in aggressive cell lines, such as breast cancer (4T1), liver cancer (HepG2, Hepa1-6), and pancreatic cancer (Pan02) cells compared with less aggressive cancer cells (Fig. 1G). These data suggested that TMEM189 may play a role in cancer progression.

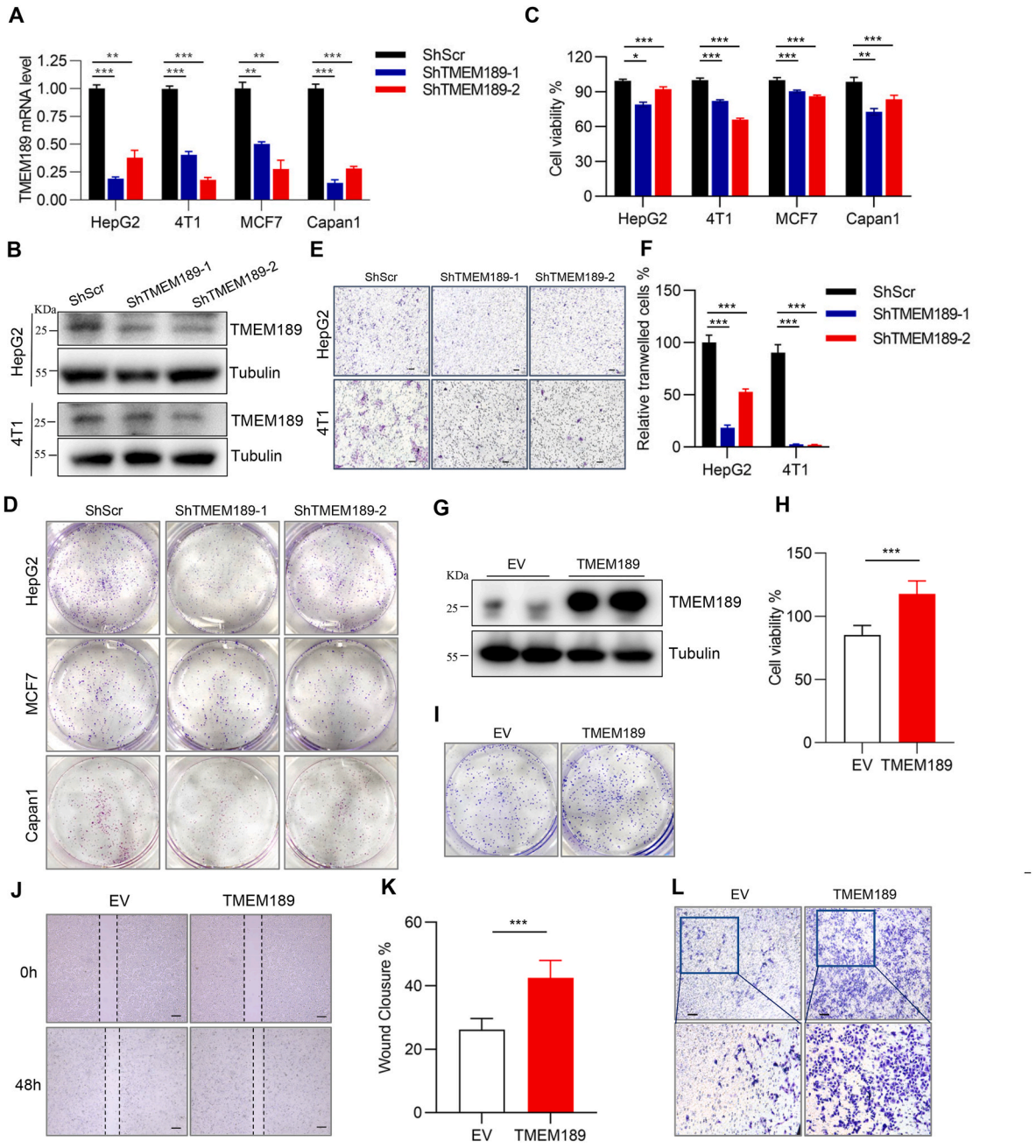

Fig. 2. TMEM189 promotes cancer cell growth and migration

(A) HepG2, MCF7, and Capan1 cells stably expressing either scramble or human TMEM189 shRNA, and 4T1 cells stably expressing either scramble or mouse TMEM189 shRNA were subjected to quantitative real-time PCR to detect knockdown efficiency (n = 3 per group). (B) HepG2 cells stably expressing either scramble or human TMEM189 shRNA, and 4T1 cells stably expressing either scramble or mouse TMEM189 shRNA were subjected to Western blotting. (C) The cells as indicated were subjected to cell viability assay as described in Method (n = 3 per group). (D) The cells as indicated were subjected to cell colony formation assay as described in Method. The whole well of 6- well plate was presented. (E) Representative images of Transwell assay (Magnification, 10×. Scale bar, 100 μm). (F) Quantitation of (E) (n = 5 per group). (G) HepG2 cells stably expressing either empty vector (EV) or human TMEM189 were subjected to Western blotting. (H) Cell viability assay was performed for HepG2 cells stably expressing either empty vector (EV) or human TMEM189. (I) Colony formation assay was performed for HepG2 cells stably expressing either empty vector (EV) or human TMEM189. The whole well of 6- well plate was presented. (J–K) The migration ability of HepG2 cells stably expressing either empty vector (EV) or human TMEM189 was assessed by wound-healing assay. Photographs were taken at 0 and 48 h following the initial scratch. Migration rates were quantified by measuring three different wound areas (n = 3) (Magnification, 10×. Scale bar, 100 μm). Three separate experiments were performed. (***$p < 0.001$). (L) Transwell assay was performed for HepG2 cells stably expressing either empty vector (EV) or human TMEM189. (Magnification, 10×. Scale bar, 100 μm).Data were shown as the means ± SEM. *$p < 0.05$, **$p < 0.01$ and ***$p < 0.001$.

3.2. The intervention of TMEM189 modulates cancer cell growth and migration

To determine the role of TMEM189 in cancer cells, we inhibited TMEM189 expression using shRNA in breast (4T1, and MCF-7), liver (HepG2), and pancreatic (Capan-1) cancer cell lines (Fig. 2A and B). The cell viability analysis and colony formation assay demonstrated that the knockdown of TMEM189 could inhibit the growth of MCF-7, HepG2, and Capan-1 (Fig. 2C and D). Besides, the reduction of TMEM189 also resulted in a significant decrease in cell migration and invasion of 4T1

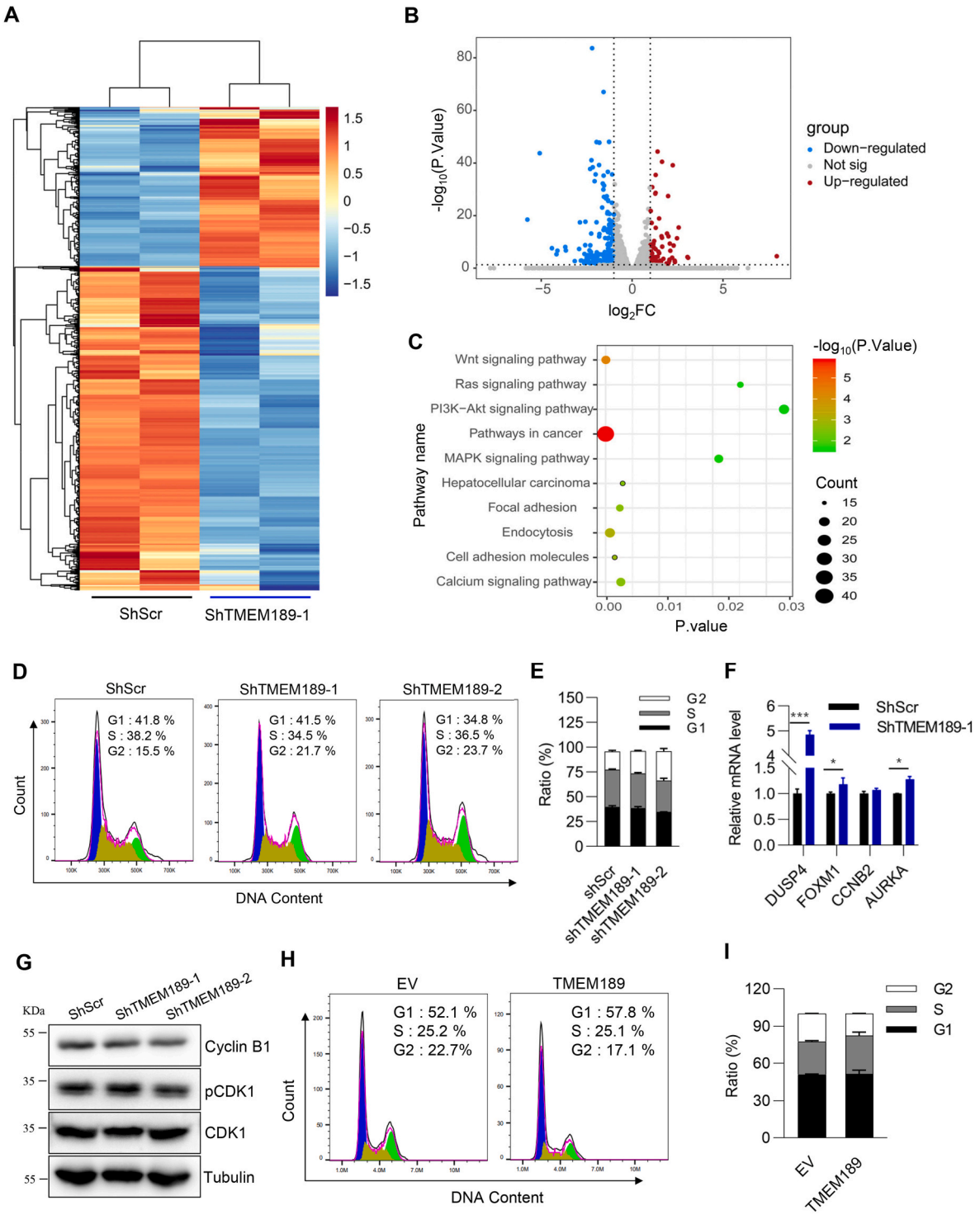

Fig. 3. TMEM189 deficiency inhibits cancer cell proliferation by inducing G2/M arrest

(A-C) HepG2 cells stably expressing either scramble or TMEM189 shRNA were subjected to transcriptomic analysis. (A) Heatmap and (B) Volcano map presented a total of 1052 genes differentially expressed, including 345 upregulated and 707 downregulated genes. (C) KEGG pathway analysis of differentially expressed genes. Advanced bubble chart shows enrichment of differentially expressed genes in signaling pathways. (D–E) Flow cytometry analysis and quantification were performed to check cell cycle phases of HepG2 cells stably expressing either scramble or TMEM189 shRNA (n = 3). (F) The mRNA levels of G2/M arrest-related markers were detected by quantitative real-time PCR in HepG2 cells stably expressing either scramble or TMEM189 shRNA. (G) The protein levels of G2/M arrest-related markers were detected by Western blot in HepG2 cells stably expressing either scramble or TMEM189 shRNA. (H–I) Flow cytometry analysis and quantification were performed to check cell cycle phases of HepG2 cells stably expressing either empty vector (EV) or TMEM189 (n = 3). Data were shown as the means ± SEM. $*p < 0.05$, $**p < 0.01$ and $***p < 0.001$.

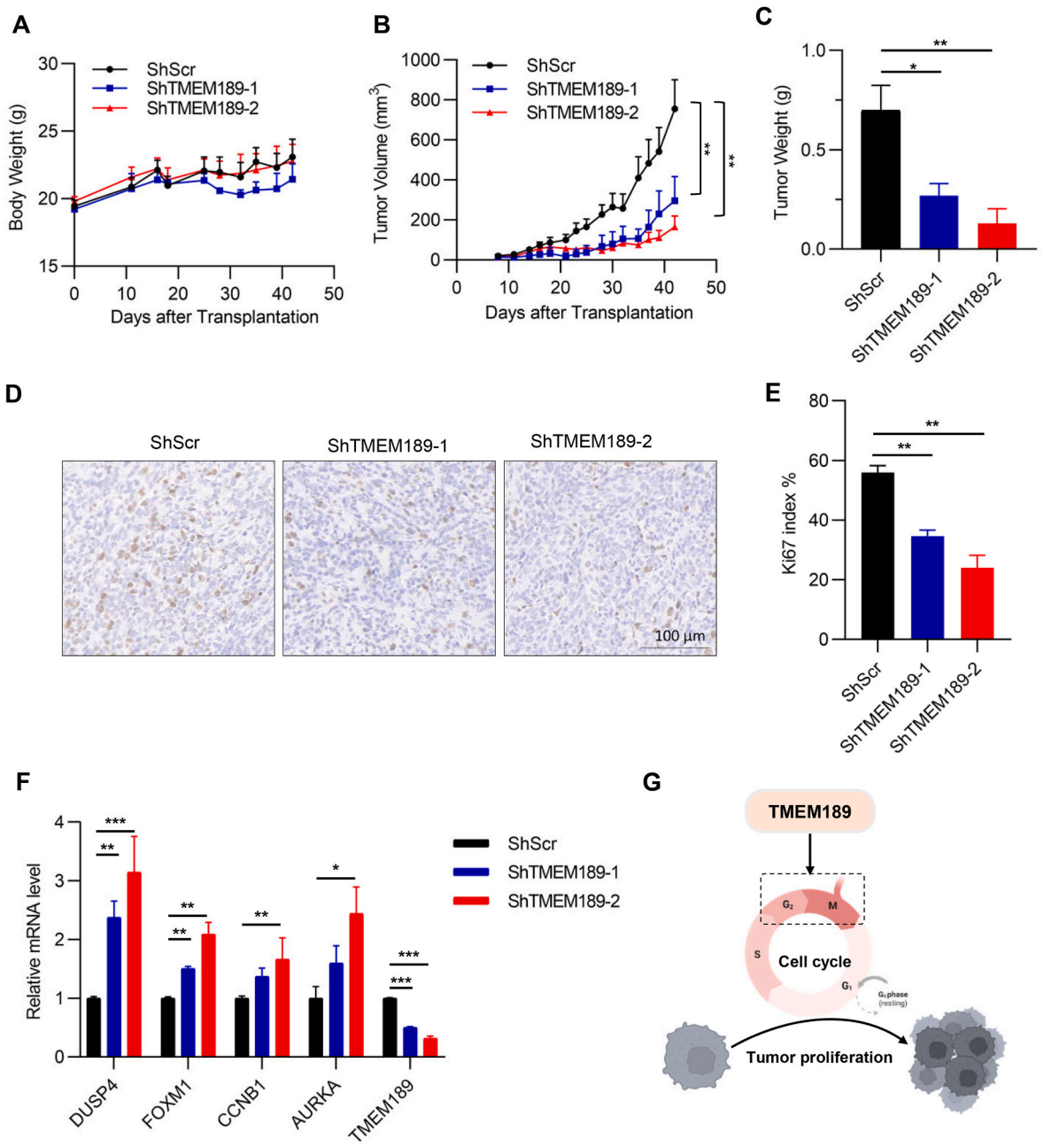

Fig. 4. Deletion of TMEM189 inhibits the growth of breast cancer *in vivo*

(A-F) 4T1 cells stably expressing either scramble or mouse TMEM189 shRNA were subcutaneously injected on both sides of the dorsum of the BALB/c mice in a total volume of 100 μL (2×10^4 cells/mouse). (A) The growth rate of xenografted mice. (B) Tumor volumes (tumor volume = width^2 × length × 1/2). (C) Tumors were isolated and weighed at the endpoint of experiments. (D) Representative images of tumor sections stained with Ki67 antibody. (E) The percentage of Ki67 positive cells. (F) The mRNA levels of G2/M arrest markers were detected by RT-PCR for tumor samples (n = 8). (G) Schematic model of the role of TMEM189 in tumor proliferation. Data were shown as the means ± SEM. *$p < 0.05$, **$p < 0.01$ and ***$p < 0.001$.

and HepG2 cancer cells as assessed by Transwell assay (Fig. 2E and F). By contrast, overexpression of TMEM189 promoted the growth of HepG2 cells as assessed by cell viability and colony formation assays (Fig. 2G–I). TMEM189 overexpression also significantly elevated HepG2 cell motility as assessed by wound healing and Transwell assays (Fig. 2J-L). Taken together, our data demonstrated that TMEM189 exacerbates the aggressiveness of cancer cells.

3.3. *TMEM189 depletion leads to G2/M arrest*

To determine the molecular mechanism underlying the effect of TMEM189 inhibition on the growth and migration of cancer cells, we subjected HepG2 cells stably expressed either scramble or TMEM189 shRNA to the transcriptomic analysis. A total of 1052 genes were differentially expressed, including 345 upregulated and 707 down-regulated genes (Fig. 3A and B). Then all the genes that were down-regulated more than 2-fold were selected to commit the pathway enrichment analysis. The results of GO enrichment analysis demonstrated that the differentially expressed genes were significantly enriched in cell growth and proliferation-related pathways, such as Ras signaling pathway, MAPK signaling pathway, and PI3K-Akt signaling pathway (Fig. 3C). Together, our data suggested that TMEM189 may function as an oncogene through regulating cell proliferation-related pathways in hepatic cancer cells.

To further determine how TMEM189 affects cell proliferation, we performed propidium iodide staining followed by FACS analysis to determine the cell cycle distribution. Knockdown of TMEM189 induced an increase of cell counts in the G2/M phase compared to the control group (Fig. 3D and E). In line with this observation, the markers of G2/M arrest, such as DUSP4, AURKA, FOXM1, and CCNB2 [15,16], were upregulated in TMEM189 knockdown cells (Fig. 3F). Besides, Western blot analysis of key protein molecules *p*-CDK1 and cyclin B1, which are related to the G2-M transition of the cell cycle, were decreased in TMEM189 knockdown cells (Fig. 3G). By contrast, we observed that TMEM189 overexpression led to a lower cell count of the G2/M phase in HepG2 cells (Fig. 3H and I). In summary, our results indicated that TMEM189 depletion might suppress cancer cell proliferative capacity by arresting the cell cycle at the G2/M phase.

3.4. *TMEM189 depletion suppresses the growth of breast tumors in vivo*

To test whether targeting TMEM189 could prevent tumor growth *in vivo*, we constructed a breast cancer xenograft model by subcutaneous injection of 4T1 cells stably expressing scramble or TMEM189 shRNA into 8-week-old BALB/C mice. Of note, body weights were comparable between the two groups (Fig. 4A). Remarkably, the tumor volume curves demonstrated that the xenografts of the shTMEM189 group grew significantly slower than the control group at the site of injection within the experimental period (Fig. 4B). In line with this observation, the tumor weights were significantly lower in the TMEM189 knockdown group compared to the scramble group (Fig. 4C). Immunohistology analysis showed that the tumors derived from the TMEM189 knockdown group revealed a lower number of Ki67-positive cells than those from the scramble group (Fig. 4D and E). In agreement with the findings *in vitro*, the markers of G2/M arrest were dramatically increased in TMEM189 knockdown tumors (Fig. 4F). Collectively, depletion of TMEM189 leads to cell cycle G2/M arrest and the suppression of breast tumor growth (Fig. 4G), indicating that TMEM189 is a potential therapeutic target for breast cancer.

4. Discussion

Here we demonstrated that the expression level of TMEM189 was negatively correlated with the survival rate of cancer patients. The depletion of TMEM189 in liver, breast, and pancreatic cancer cell lines suppressed cell proliferation and migration. Furthermore, we found that TMEM189 promoted cell proliferation by regulating cell cycle G2/M phase transition both *in vitro* and *in vivo*. Knockdown of TMEM189 suppressed the growth of breast tumors *in vivo*, indicating that TMEM189 was a potential therapeutic target for breast cancer.

Lipid metabolism reprogramming is a major hallmark of cancer cells. Lipid is not only building blocks that constitute cells, but also important signaling molecules for many cellular activities [17]. TMEM189, also called plasmanylethanolamine desaturase 1 (PEDS1), is required for the biosynthesis of ethanolamine plasmalogen—a special phospholipid. For evidence, TMEM189 deletion could lead to the lack of plasmalogens in mouse kidney [8]. Interestingly, in gastric carcinoma patients, the plasma plasmalogen content was significantly elevated compared to normal groups [18], suggesting that TMEM189 might regulate cancer cell growth via plasmalogen.

The acquired capability of sustaining proliferative signaling is regulated by several important pathways in cancer cells, including Ras signaling, JAK/STAT signaling, PI3K/AKT signaling and WNT/APC signaling [19,20]. In our RNAseq data, the top 3 upregulated pathways are WNT signaling, RAS signaling, and AKT-PI3K signaling, indicating that TMEM189 plays a role in tumor proliferation (Fig. 3C). The alterations of some key molecules in cell cycle checkpoints are tightly associated with tumor cell proliferation, such as cyclin-dependent kinases. These kinases control the progression through the different phases of the cell division cycle [21]. Induction of G2/M arrest suppresses cell proliferation and targeting G2/M transition is a promising strategy to treat cancer [22,23]. We found that TMEM189 depletion leads to G2/M arrest, but how TMEM189 affects cell cycle transition needs further investigation.

Interestingly, TMEM189 might function independently of its plasmalogen synthetic activity, for example, TMEM189 regulates autophagy by modulating the formation of autophagosomes via direct interaction with ULK1 [10]. Autophagy, a cellular machine removing the damaged organelle, aggregates, and proteins, plays a critical role in cell homeostasis [24]. For instance, the inhibition of autophagy promotes G2/M arrest in both hepatocyte and proximal epithelial cells [25,26]. Whether TMEM189 regulate G2/M transition in an autophagy dependent manner remains to be determined.

In summary, our data suggested that TMEM189 promotes cancer progression most likely via the regulation of cell cycle G2/M transition, although the detailed mechanism still requires further investigation.

Funding

This work was supported by National Natural Science Foundation of China (32370738 to A.H.), and Natural Science Foundation of Anhui Province (2108085MC81 to A.H., 2208085QH248 to Y.C.)

CRediT authorship contribution statement

Song Chen: Data curation, Formal analysis, Investigation. **Meng Tie:** Formal analysis, Investigation. **Mengyue Wu:** Investigation. **Anyuan He:** Formal analysis, Funding acquisition, Supervision, Writing – review & editing. **Yali Chen:** Funding acquisition, Investigation, Project administration, Supervision, Validation, Writing – original draft, Writing – review & editing.

Declaration of competing interest

The authors declare that they have no known competing financial interests or personal relationships that could have appeared to influence the work reported in this paper.

Data availability

Data will be made available on request.

Acknowledgment

The authors are thankful to Dr. Yunzhi Yang and Dr. Yong Chen for their critical comments on this manuscript.

Appendix A. Supplementary data

Supplementary data to this article can be found online at https://doi.org/10.1016/j.bbrep.2024.101744.

References

[1] N.N. Pavlova, C.B. Thompson, The emerging hallmarks of cancer metabolism, Cell Metabol. 23 (2016) 27–47.
[2] L. Yin, J.J. Duan, X.W. Bian, S.C. Yu, Triple-negative breast cancer molecular subtyping and treatment progress, Breast Cancer Res. 22 (2020).
[3] D. Hanahan, Hallmarks of cancer: new dimensions, Cancer Discov. 12 (2022) 31–46.
[4] D. Yan, Q. He, L. Pei, M. Yang, L. Huang, J. Kong, W. He, H. Liu, S. Xu, H. Qin, T. Lin, J. Huang, The APC/C E3 ligase subunit ANAPC11 mediates FOXO3 protein degradation to promote cell proliferation and lymph node metastasis in urothelial bladder cancer, Cell Death Dis. 14 (2023) 516.
[5] S. Kulkarni, Q. Li, A.D. Singhi, S. Liu, S.P. Monga, A.P. Feranchak, TMEM16A partners with mTOR to influence pathways of cell survival, proliferation, and migration in cholangiocarcinoma, Am. J. Physiol. Gastrointest. Liver Physiol. 325 (2023) G122–g134.

[6] E.H. Maleki, A.R. Bahrami, M.M. Matin, Cancer cell cycle heterogeneity as a critical determinant of therapeutic resistance, Genes & diseases 11 (2024) 189–204.
[7] A.D. McAinsh, G. Kops, Principles and dynamics of spindle assembly checkpoint signalling, Nat. Rev. Mol. Cell Biol. 24 (2023) 543–559.
[8] E.R. Werner, M.A. Keller, S. Sailer, K. Lackner, J. Koch, M. Hermann, S. Coassin, G. Golderer, G. Werner-Felmayer, R.A. Zoeller, N. Hulo, J. Berger, K. Watschinger, The TMEM189 gene encodes plasmanylethanolamine desaturase which introduces the characteristic vinyl ether double bond into plasmalogens, Proceedings of the National Academy of Sciences of the United States of America 117 (2020) 7792–7798.
[9] A. Gallego-García, A.J. Monera-Girona, E. Pajares-Martínez, E. Bastida-Martínez, R. Pérez-Castaño, A.A. Iniesta, M. Fontes, S. Padmanabhan, M. Elías-Arnanz, A bacterial light response reveals an orphan desaturase for human plasmalogen synthesis, Science (New York, N.Y.) 366 (2019) 128–132.
[10] J. Yu, L. Qu, Y. Xia, X. Zhang, J. Feng, M. Duan, P. Guo, Y. Lou, P. Lv, W. Lu, Y. Chen, TMEM189 negatively regulates the stability of ULK1 protein and cell autophagy, Cell Death Dis. 13 (2022) 316.
[11] S.A. Stewart, D.M. Dykxhoorn, D. Palliser, H. Mizuno, E.Y. Yu, D.S. An, D. M. Sabatini, I.S. Chen, W.C. Hahn, P.A. Sharp, R.A. Weinberg, C.D. Novina, Lentivirus-delivered stable gene silencing by RNAi in primary cells, RNA (New York, N.Y.) 9 (2003) 493–501.
[12] X. Lu, Y. Zhu, R. Bai, Z. Wu, W. Qian, L. Yang, R. Cai, H. Yan, T. Li, V. Pandey, Y. Liu, P.E. Lobie, C. Chen, T. Zhu, Long-term pulmonary exposure to multi-walled carbon nanotubes promotes breast cancer metastatic cascades, Nat. Nanotechnol. 14 (2019) 719–727.
[13] W. Zhao, L. Zhang, Y. Zhang, Z. Jiang, H. Lu, Y. Xie, W. Han, W. Zhao, J. He, Z. Shi, H. Yang, J. Chen, S. Chen, Z. Li, J. Mao, L. Zhou, X. Gao, W. Li, G. Tan, B. Zhang, Z. Wang, The CDK inhibitor AT7519 inhibits human glioblastoma cell growth by inducing apoptosis, pyroptosis and cell cycle arrest, Cell Death Dis. 14 (2023) 11.
[14] M.I. Love, W. Huber, S. Anders, Moderated estimation of fold change and dispersion for RNA-seq data with DESeq2, Genome biology 15 (2014) 550.
[15] P. Ratsada, N. Hijiya, S. Hidano, Y. Tsukamoto, C. Nakada, T. Uchida, T. Kobayashi, M. Moriyama, DUSP4 is involved in the enhanced proliferation and survival of DUSP4-overexpressing cancer cells, Biochemical and biophysical research communications 528 (2020) 586–593.
[16] F. He, L. Antonucci, S. Yamachika, Z. Zhang, K. Taniguchi, A. Umemura, G. Hatzivassiliou, M. Roose-Girma, M. Reina-Campos, A.D. Molina, NRF2 activates growth factor genes and downstream AKT signaling to induce mouse and human hepatomegaly, J. Hepatol. (2020).
[17] X. Bian, R. Liu, Y. Meng, D. Xing, D. Xu, Z. Lu, Lipid metabolism and cancer, J. Exp. Med. 218 (2021).
[18] J. Lv, C.Q. Lv, L. Xu, H. Yang, Plasma content variation and correlation of plasmalogen and gis, tc, and tpl in gastric carcinoma patients: a comparative study, Med Sci Monit Basic Res 21 (2015) 157–160.
[19] D. Hanahan, R.A. Weinberg, The hallmarks of cancer, Cell 100 (2000) 57–70.
[20] D. Hanahan, R.A. Weinberg, Hallmarks of cancer: the next generation, Cell 144 (2011) 646–674.
[21] M. Malumbres, Cyclins and related kinases in cancer cells, Journal of B.U.ON. : official journal of the Balkan Union of Oncology 12 (Suppl 1) (2007) S45–S52.
[22] X. Zhang, L. Geng, L. Yang, Y. Wang, Z. Zou, Y. Zhang, H. Xu, H. Lei, Y. Cao, Y. Wu, W. Gu, L. Zhou, Anlotinib exerts an anti-T-cell acute lymphoblastic leukemia effect in vitro and in vivo, Cell. Signal. (2023) 110837.
[23] E.A. Sobh, M.A. Dahab, E.B. Elkaeed, A.A. Alsfouk, I.M. Ibrahim, A.M. Metwaly, I. H. Eissa, Discovery of new thieno[2,3-d]pyrimidines as EGFR tyrosine kinase inhibitors for cancer treatment, Future Med. Chem. (2023).
[24] J.M.M. Levy, C.G. Towers, A. Thorburn, Targeting autophagy in cancer, Nat. Rev. Cancer 17 (2017) 528–542.
[25] B. Han, Y. Chen, C. Song, Y. Chen, D. Ferguson, Y. Yang, A. He, Autophagy modulates the stability of Wee1 and cell cycle G2/M transition, Biochemical and biophysical research communications 677 (2023) 63–69.
[26] H. Li, X. Peng, Y. Wang, S. Cao, L. Xiong, J. Fan, Y. Wang, S. Zhuang, X. Yu, H. Mao, Atg5-mediated autophagy deficiency in proximal tubules promotes cell cycle G2/M arrest and renal fibrosis, Autophagy 12 (2016) 1472–1486.